The 14th International Topical Meeting on Nuclear Reactor Thermalhydraulics, NURETH-14
Toronto, Ontario, Canada, September 25-30, 2011

NURETH14-532

ULTRAFAST ELECTRON BEAM X-RAY CT FOR TWO PHASE FLOW PHENOMENA

F. Barthel, D. Hoppe, L. Szalinski and U. Hampel
Helmholtz-Zentrum Dresden-Rossendorf , Dresden, Germany

Abstract

Ultrafast electron beam X-ray CT is a fast imaging technique which can be used to vizualise phase distributions in transient two-phase flows. This is important e.g. in nuclear reactor thermal hydraulics where an optical access to the flow is not feasible. Ultrafast electron beam X-ray tomography achieves frame rates of several thousand slice images per second at ~ 1 mm spatial resolutionh. From data sets several parameters whic characterize the flow, such as radial gas fraction profiles or bubble size distributions, can be extracted. This paper introduces the tomography system and presents first results obtained for upward cocurrent air-water two-phase flow experiments at the TOPFLOW facility.

Introduction

Two-phase flows are of primary importance in the understanding of thermal hydraulic phenomena in nuclear light water reactors. The qualification of CFD codes to simulate stationary and even transient two-phase flows in complex three-dimensional geometries requires extending our knowledge toward the details of the flow structure under various thermal hydraulic conditions. It is commonly accepted that validation of CFD codes requires high resolution flow data. This concerns phase distributions as well as liquid velocities, turbulence, and temperature distributions.
In the past researchers developed various sensors and measurement techniques to study two-phase flow in pipes. Simple optical and electrical sensors can give local or cross-sectional averaged information on the gas and liquid fraction. Such probes are often fast and can resolve many temporal flow details. However, they rarely give spatial flow details, have difficulties with exact parameter quantification and are intrusive. Radiation densitometry is another common technique for phase fraction measurement. It utilizes hard X-rays or gamma rays whose attenuation in the flow gives a measure of the gas-to-liquid ratio passing the radiation beam. Such type of densitometry can be quite accurate and is also non-intrusive, but on the other hand it is slow and gives no local flow information. In the past imaging techniques have become very attractive for two-phase flow studies. Worth mentioning are electrical tomography, wire mesh sensors, and radiation based computed tomography methods. Electrical tomography (*Williams, 1995*) allows getting cross-sectional images of conductivity or permittivity in the flow cross-sections with up to 1000 images per second. The simple concept is compromised by low spatial resolution. Wire mesh sensors (*Prasser et al., 1998*) have frequently been used for gas-liquid two-phase flow studies. They have a very high temporal and good spatial resolution, but are intrusive. Radiation based tomography methods are commonly slow, but can measure time-averaged phase fraction distributions with high accuracy and non-intrusively. Recently, there was some progress to

enhance the acquisition speed of radiation tomography modalities. Examples are the University of Bergen fast gamma ray tomography scanner, and ultrafast X-ray tomography (*Johansen, 2010*).
Ultrafast electron beam X-ray tomography is a young imaging technique which allows scanning flows in vessels or pipes of moderate size with speeds well above 1000 frames per second. The ultrafast electron beam tomography system ***ROFEX*** (*RO*ssendorf *f*ast *e*lectron beam *X*-ray tomograph) has been developed to study the gas liquid flow in a vertical test section at the TOPFLOW test facility at Helmholtz-Zentrum Dresden-Rossendorf. Recently upward adiabatic two-phase air-water pipe flows studies in a DN50 test section were performed. In this paper the tomography system is introduced and essential operating parameters are discussed. Examples for some selected experimental results are shown and discussed. The paper is organized as follows. Section 1 gives a brief overview on the imaging modality of the ultrafast electron beam X-ray tomography system. Section 2 describes the experimental setup. In section 3 experimental results are presented and discussed.

1. Ultrafast electron beam X-ray tomography system

1.1 Scanner design

Figure 1 shows the operation principle and a photo of the ultrafast electron beam X-ray tomograph ***ROFEX*** (*Ro*ssendorf *f*ast *e*lectron beam *X*-ray tomograph) (*Fischer, 2008).* This scanner was developed for multiphase flow studies carried out at the thermal hydraulic test facility TOPFLOW. The working principle is as follows. An electron beam of sufficient energy is produced by an electron beam gun, focussed onto a semicircular X-ray production target, which surrounds the test section. The electron beam is swept rapidly across the target by means of an electromagnetic deflection system and that way X-rays are generated from a moving focal spot. Radiation that passes the object of investigation is recorded by a fast X-ray detector. The detector is designed as a circular ring and mounted stationary inside the scanner head with some axial offset relative to the focal spot path. On the contrary to medical electron beam tomography, the setup is optimized with respect to ultrafast imaging, which implies a smaller source-detector separation and shorter electron path, accordingly.

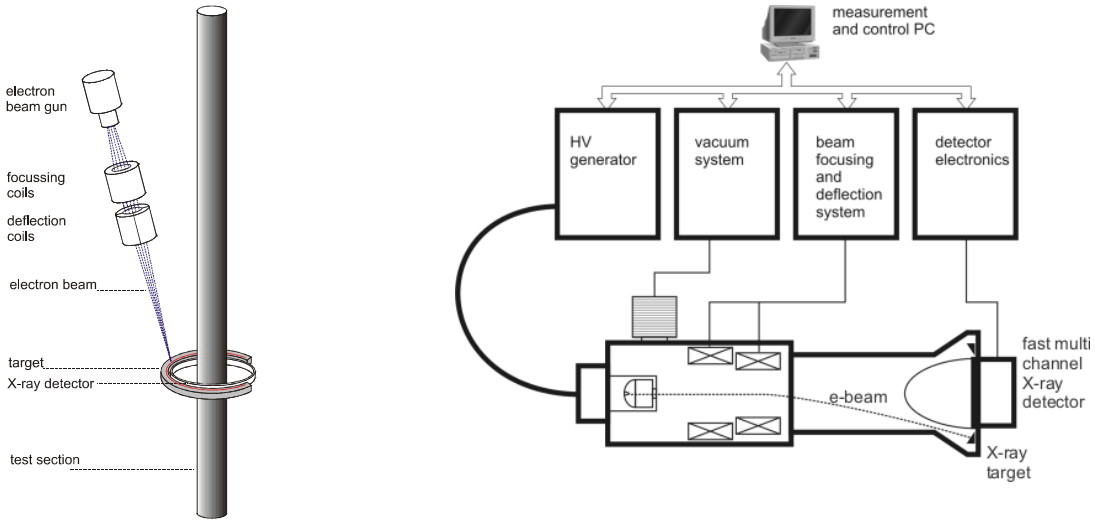

Fig. 1: left side: *working principle of ROFEX;* ***right side****: Block scheme of tomography-system*

The tomography system can be subdivided into three main parts: 1) the scanner, that comprises the high voltage generator and the electron beam gun including beam optics, the beam tube and the scanner head with the target. 2) fast x-ray detector and 3) control and beam monitoring equipment. The high-voltage generator provides the electron acceleration voltage of 150 kV at a maximum beam current of 65 mA (10 kW maximum electron beam power) along with all necessary auxiliary supplies, such as the Wehnelt voltage, surge voltage and a filament heating current. The electron beam gun is kept at 10^{-6} mbar pressure by means of vacuum pumps and controllers. The accelerated electrons pass the beam forming and centring section and the beam is focussed to a small focal spot (about 1 mm) on the target by means of deflection coils, producing a circular focal spot path. The X-ray target is a semicircular metal ring (240° opening angle) residing in the scanner head. The fast X-ray detector is arranged inside the opening with a slight axial offset of 3 mm relative to the focal spot plane. It consists of 240 room-temperature semiconductor detector pixels with an active area of 1.33 x 1.33 mm. These pixels generate a current proportional to the received X-ray flux. This current is converted into a voltage, amplified and eventually digitalized by 12 bit ADCs. These signals are transferred and stored in a 4GB SDRAM for 512 channels maximum synchronously. At maximum sampling rate of 1 MSamples/s an acquisition time duration of about 10 seconds is possible. After each measurement scan the data are transferred to a PC via a USB 2.0 connection and can be reconstructed. Figure 2, left side shows the block scheme of the detector electronics. Beam monitoring is done using a vision system that allows assessing the focal spot quality as well as proper positioning of the beam on the target. The deflection pattern for steering the electron beam is controlled by the PC and the detector data acquisition and image reconstruction software is implemented in C++. For further detailed descriptions see *Fischer, 2008*.

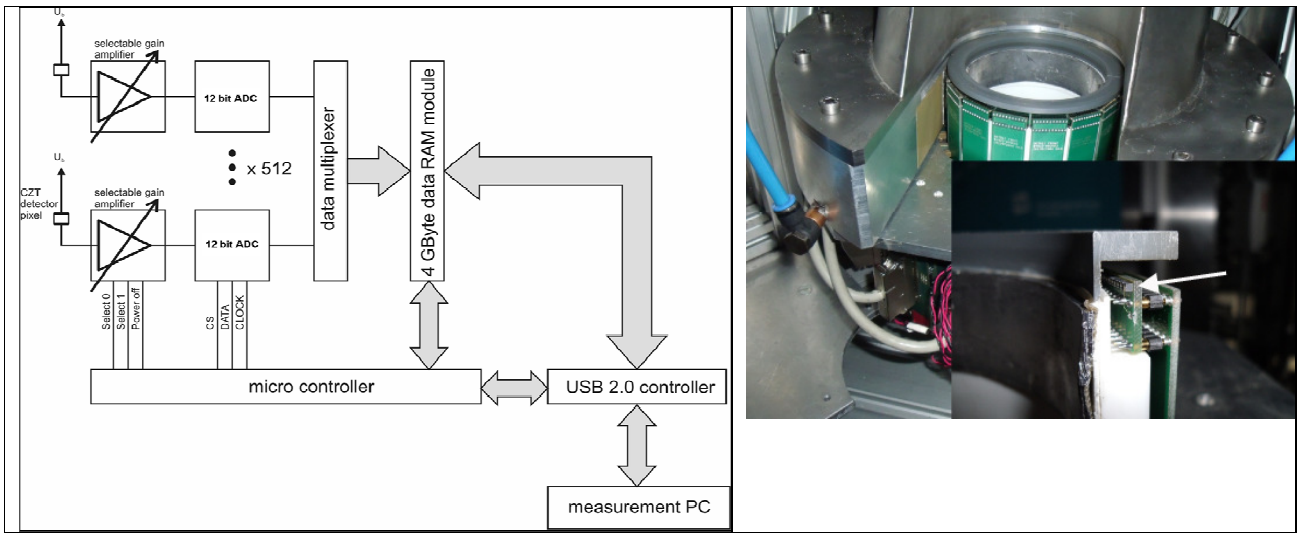

Figure 2: left side: block scheme of detector electronics; ***right side:*** Photograph of tomograph´s head with the X-ray detector (white arrow points at pixel row).

1.2 Data processing

Once a scan has been performed and data has been transferred to the PC the data is pre-processed and reconstructed according to the classical image reconstruction principles of tomography (*Kak et al., 1988*). The raw data is given by the binary detector readings, that is, 240 12-bit integer values for each temporal sampling step of the detector. This data sequence is first broken into sets of size $N_D \times N_T$ where N_D=240 is the number of detectors and N_T the number of equidistant temporal points for a complete electron beam revolution. Next the data of each frame is mapped from the temporal domain into the angular domain of the target. That is, we calculate a projection data matrix of size $N_D \times N_S$ where N_S is the number of equidistantly distributed source positions on the target. Note, that this transformation is a comparatively complex nonlinear one, which is necessary due to the fact that the source trajectory on the target is a cut of a skewed elliptical cone. Now the data can be resorted into a fan beam data set as for a conventional tomography scanner. Thereby, we discard all data from source positions outside the valid angular scanning range of 240°. For the fan beam data of each frame the line integral X-ray attenuation values are calculated according to

$$E_{i,j} = -\log \frac{I_{i,j} - I_{i,j}^{(d)}}{I_{i,j}^{(0)} - I_{i,j}^{(d)}} \tag{1}$$

Here, I denotes X-ray intensity, i and j are the indices of detector and projection, superscript *(d)* denotes a previously acquired dark reference and (0) a previously acquired reference measurement with no object in the tomographic cross-section. Eventually the data is reconstructed by the fan-beam reconstruction algorithm. In our software implementation we reconstruct the data on a 128 x 128 pixel grid using a Hamming window smoothed ramp filter for restoring the image from the unfiltered backprojection. Data processing and image reconstruction takes about 2 s for one frame. Thereby the scanner allows us to scan the flow for as much as 10 s overall time with a temporal resolution of 1000 frames per second. Thus, the data is acquired at full speed and data processing needs to be performed in an offline mode after the scan. Figure 3 shows geometry in the tomography plane. Objects up to 120 mm diameter can be scanned.

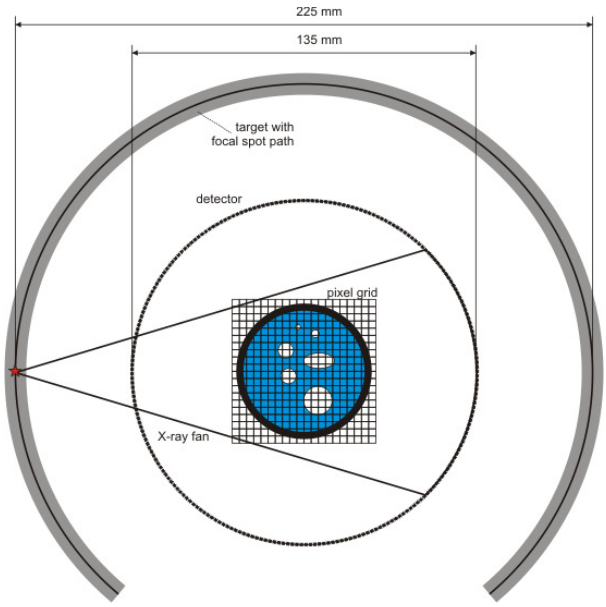

Figure 3: *Geometric conditions in the scanning plane*

1.3 Scanner performance

Spatial resolution within the reconstructed images has been determined from the edge of a drill in a scanned object as shown in figure 4. It shows the modulation transfer function from a grey value profile along a horizontal line through one of the drills of the object. As a result we obtain a value for the spatial resolution of the scanner of 0.51 line pairs per millimetre at 10% MTF.

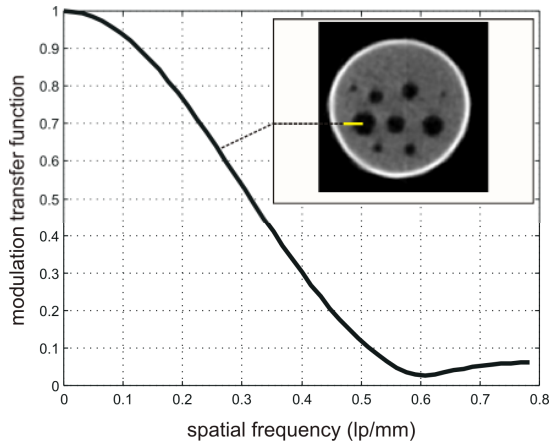

Figure 4: *Modulation transfer function obtained from a reconstructed object edge.*

Beside the spatial resolution, which is independent of contrast, one has to account for contrast when it comes to detectability of structures. For two-phase flow this concerns the smallest gas bubble which can be securely discriminated by automatic algorithms. Limitation of contrast is due to two effects: firstly, there is a 12 bit (4096 step) limit of the detectors's analogue-to-digital converters. Secondly contrast is limited by signal-to-

noise ratio, which is mainly determined by photon statistics in the short integration time windows. Experimentally we found that for gas-water two-phase flow this contrast/resolution limit is roughly 2 mm.

2. Experimental setup

This paper introduces two-phase gas-liquid flow measurements at the TOPFLOW facility (Transient Two-Phase Flow Test Facility) at HZDR. Targets of these studies are air-water and steam-water two-phase flows in a vertical pipe with an inner diameter of about 50 mm (DN50). Figure 6 shows the test section, tomography scanner and gas injection. The objective is the investigation of the flow evolution along the pipe for different gas and liquid superficial velocities and a comparison of steam-water with air-water flows. The new X-ray tomography scanner now for the first time enables to perform a quasi-continuous axial measurement of phase fraction distributions with no intrusion and corresponding flow disturbance. To perform measurements with the scanner a vertical manipulator has been erected around the test section, which can lift the scanner into any required measurement position along the 4.2 m lengths of the pipe. The manipulator includes an elevating system driven by a stepper motor and a mounting bracket to hold the tomography scanner in position. The elevator is 1.5 m x 1.5 m wide and 6 m tall. The sliding carriage can be moved from position 0.5 m to position 4.5 m. It reaches a vertical translation velocity of 0.5 meter per second maximum. For radiation protection a casing made of 6 millimetres lead walls is mounted around the scanner. To balance the resulting heavy mass a counterweight is mounted on the elevator. The test section is made of titanium alloy with 1.5 mm wall thickness, which is sufficient to withstand the nominal maximum pressure of 7 MPa inside the test section during steam experiments. The advantage of titanium over steel is its lower radiation attenuation. At the bottom a multi-hole gas injection device is installed which enables homogeneous injection of small gas bubbles across the cross-section of the pipe. The gas injection device has a complex design and is made of stainless steel. It comprises 40 cannulae which are fed with gas from several ring chambers. The ring chambers can be activated separately to adjust the gas flow rate. In between the ring shaped gas chambers the water can flow continuously. Thus we get a well rectified, homogenous gas-water flow whose flow rate can be varied. Downstream the injector the flow will develop into its characteristic flow regimes, which may be bubbly, churn, slug or annular. The X-ray tomography measurement begins directly at gas injection level. By moving the tomography scanner vertically along the pipe and scanning at arbitrarily selected levels we get complete data sets of the developing flow regimes. For data processing additional software has been implemented, which enables converting of gray values in slice images to gas fraction values. Then radial gas fraction distributions are extracted and eventually segmentation of gas bubbles and computation of bubble volume and equivalent diameter is done. These data will in the future further be used to develop and improve models for bubble force balances in bubble and churn flow and help to validate two-phase flow CFD code predictions.

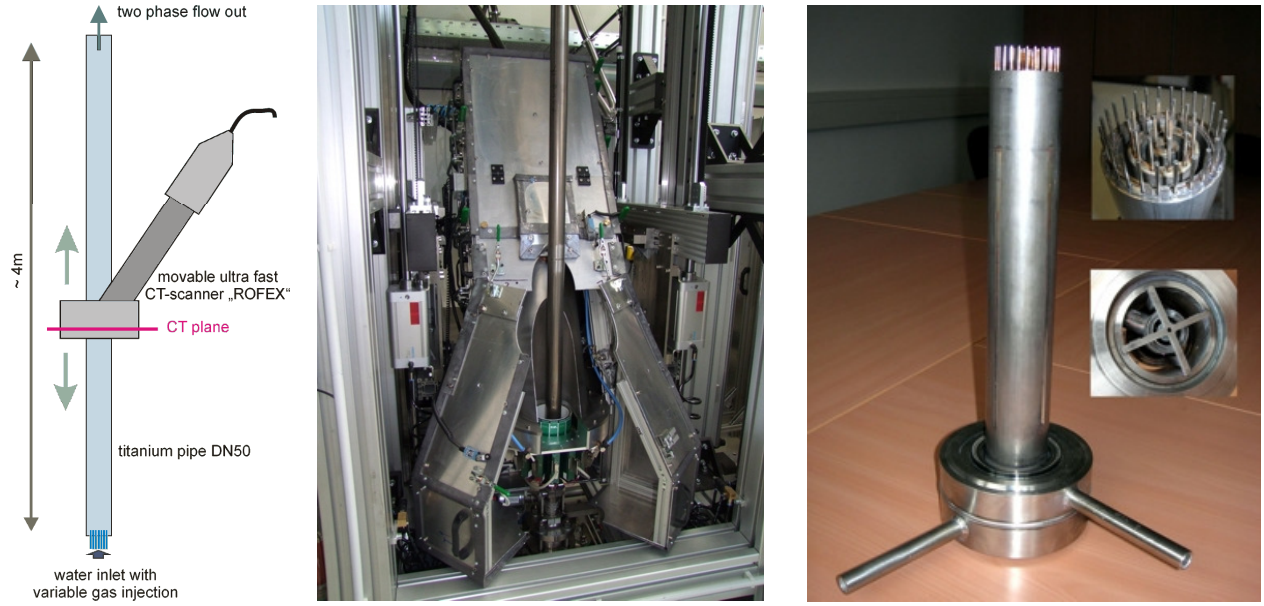

Figure 6: left side: *scheme of the titanium test section with tomography scanner and gas injection;* ***middle:*** *scanner in elevator system;* ***right side:*** *multi-hole gas injection device*

3. Experimental results

In 2010 an extensive measurement campaign for air-water flows was accomplished. In the following selected results are presented to show the performance potential of the ultrafast X-ray tomography for investigations on two phase flows. There is still some ongoing work to optimize the data evaluation procedures. For this reason the data shown here are to some extent preliminary. Two superficial velocity combinations (#50, #117) were chosen from the benchmark database (*Lucas et al., 2010*), achieved in former experiments by using the wire mesh sensor. Table 2 gives the experimental matrix with parameter combinations framed out. For the matrix point #50 the gas was feed in using three cannulae (inner chamber) only. The regime at point #117 was driven by all ring chambers (40 cannulae). For these two flow conditions data sets of slice images on different heights along the DN50 pipe were acquired with a frequency of 2500 Hz. The measuring time was 4 s. From these data sets we give axial cuts to visualize the flow regime. Furthermore we obtained bubble size distributions and radial gas fraction distributions (see Figure 7+8).

Table 2: Experimental matrix: superficial velocities for liquid vs. gas; chosen parameter combinations #50, #117 framed red.

	JG [m/s]	0,0025	0,004	0,0062	0,0096	0,0151	0,0235	0,0368	0,0574	0,0898	0,14	0,219	0,342	0,534	0,835	1,305	2,038	3,185
JL [m/s]																		
4,047		11	22	33	44	55	66	77	88	99	110	121	132	143	154	165	176	187
2,554		10	21	32	43	54	65	76	87	98	109	120	131	142	153	164	175	186
1,611		9	20	31	42	53	64	75	86	97	108	119	130	141	152	163	174	185
1,017		8	19	30	41	52	63	74	85	96	107	118	129	140	151	162	173	184
0,641		7	18	29	40	51	62	73	84	95	106	117	128	139	150	161	172	183
0,405		6	17	28	39	50	61	72	83	94	105	116	127	138	149	160	171	182
0,255		5	16	27	38	49	60	71	82	93	104	115	126	137	148	159	170	181
0,161		4	15	26	37	48	59	70	81	92	103	114	125	136	147	158	169	180
0,102		3	14	25	36	47	58	69	80	91	102	113	124	135	146	157	168	179
0,0641		2	13	24	35	46	57	68	79	90	101	112	123	134	145	156	167	178
0,0405		1	12	23	34	45	56	67	78	89	100	111	122	133	144	155	166	177

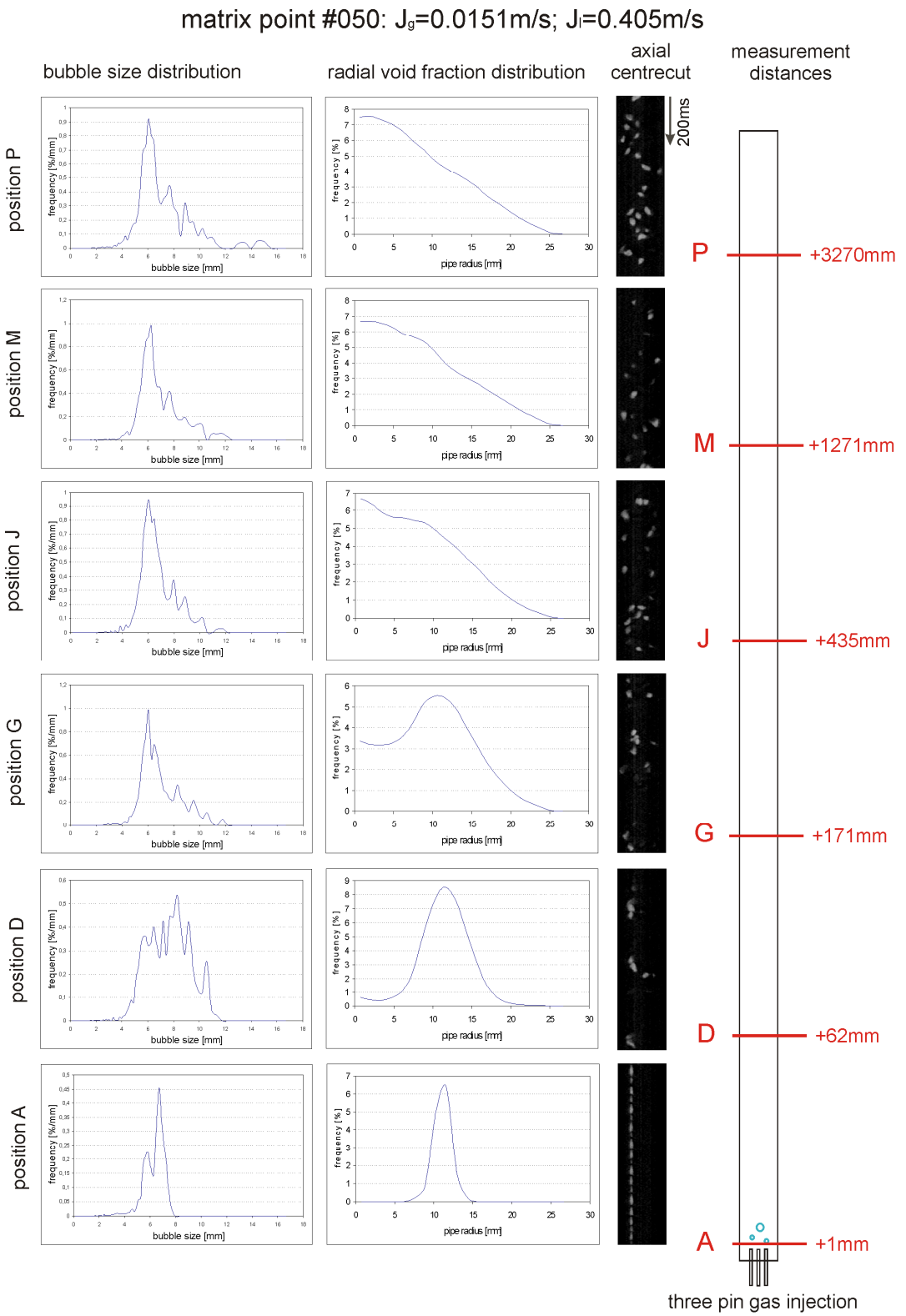

Figure 7: *Bubble size distribution and radial void fraction distribution and axial cut images for matrix point #050 at six heights. Right: Corresponding scanning planes.*

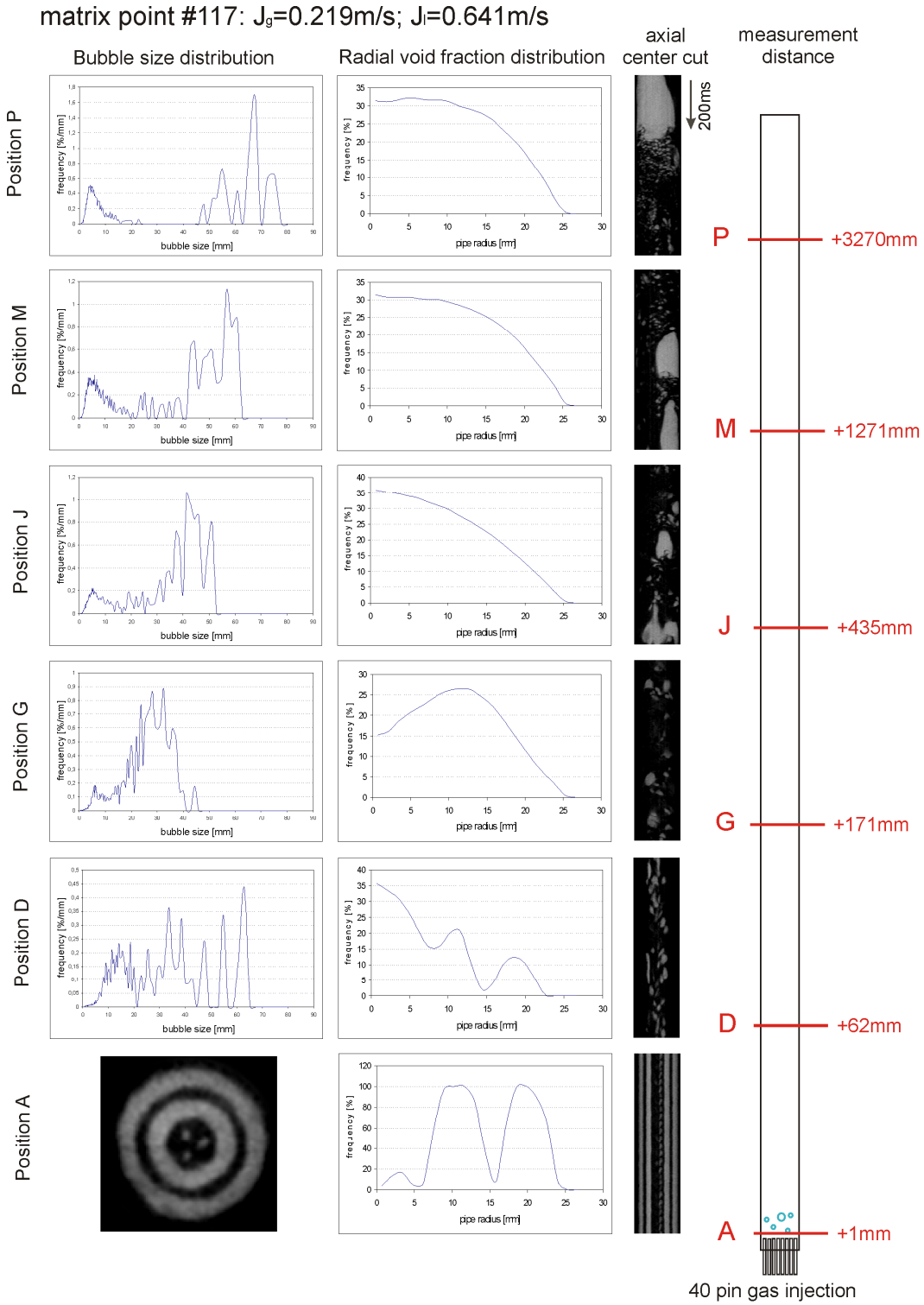

Figure 8: *Bubble size distribution and radial void fraction distribution and axial cut images for matrix point #117 at six heights. Right: Corresponding scanning planes.*

Obviously matrix point #050 leads to bubbly flow whereas #117 represents typical slug flow. In figure 8 there is a development in radial void fraction distribution from the clear forming of gas rings at radii where the injector cannulae rings are towards coalescing bubbles, moving to the centre of pipe. Simultaneously a multimodal bubble size distribution appears. Further post-processing and extensive data analysis are in process. A next step will be steam-water experiments at the same test section of the TOPFLOW facility for 70 bars/286°C.

Beside the extraction of flow parameters from tomographic data sets there is a unique feature using ultrafast electron beam X-ray tomography at all. Due to the non-invasive measurement technique one can access fine details of the flow that cannot be done with any other conventional measurement technique. Figure 9 shows some selected details captured by the ***ROFEX*** tomography scans.

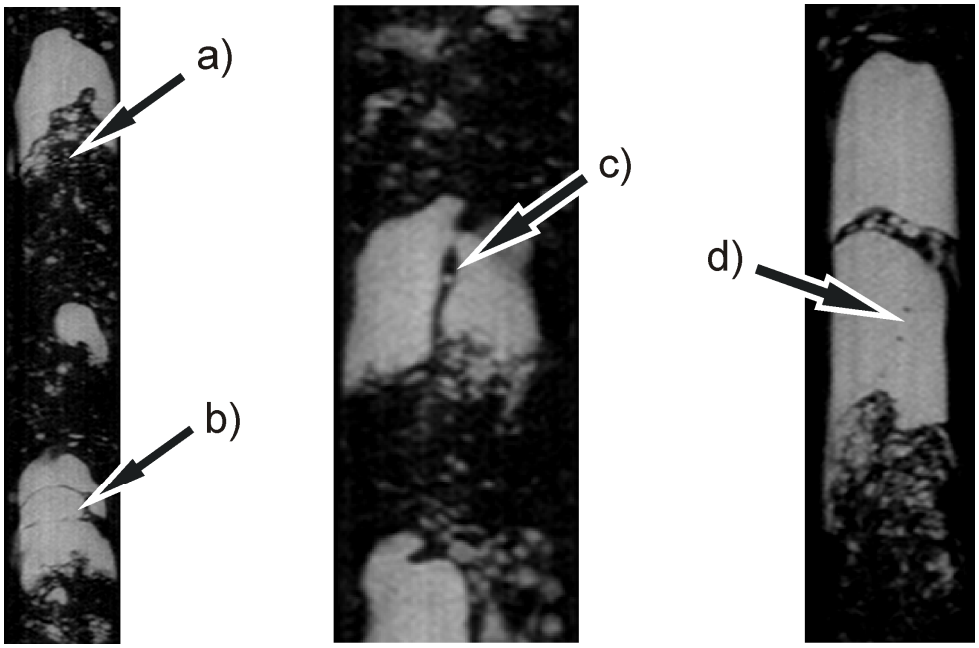

Figure 9: *axial cuts from time sequences shows details of flow;* ***a)*** *bubble cluster in the wake of large bubble;* ***b)*** *liquid lamellae separate large bubbles;* ***c)*** *single gas bubble in water hose between two bubbles;* ***d)*** *water drops in a large gas bubble*

In Figure 9 arrow *b*) points on thin water lamellae that separates three large bubbles from each other. Such data can help to enhance precision of bubble size distribution. (MUSIG [*Liao et al., 2011*]). Arrows at *c)* and *d)* points on single bubble effects not recognized in the past using wire mesh sensors due to its interaction with the flow. On the right side *(d)* one can see entrainment of few water drops inside a Taylor bubble.

4. Conclusion

Ultrafast electron beam X-ray tomography is a new imaging tool for investigations on two phase flow phenomena. Its main advantage is the non-intrusiveness enabling an observation of the undisturbed flow. Furthermore this technique gives novel possibilities to gain insight into the complex structure of two-phase flows at any gas fraction. In this paper an investigation on air-water

two phase flows in the DN50 vertical test section of the TOPFLOW facility at HZDR was done. Therefore two selected data sets of tomographic slice images of the flow evolution along the pipe at six heights were acquired. From these images radial void fraction distributions and bubble size distributions were extracted. Furthermore few visualized details of the flow which could be accessed for the first time were discussed.

5. Acknowledgements

This work is carried out in the frame of a current research project funded by the German Federal Ministry of Economics and Technology, project number 150 1329. The authors like to thank all members of the TOPFLOW team who contributed to the successful performance of these experiments.

6. References

[1] WILLIAMS R.A. and BECK M.S "Process Tomography: Principles, Techniques and Applications", Oxford, UK: Butterworth-Heinemann, (1995)

[2] PRASSER H-M, BÖTTGER A and ZSCHAU J, "A new electrode mesh tomograph for gas–liquid flows", Flow Meas. Instrum. (1998) 9 111–9

[3] JOHANSEN G.A., HAMPEL U., HJERTAKER B.T., "Flow imaging by high speed transmission tomography", Appl. Rad. Isotops, (2010) 68 518-524

[4] FISCHER F. et al., "An ultrafast electron beam x-ray tomography scanner", Measurement Science and Technology 19 (2008) 094002

[6] LUCAS, D.; BEYER, M.; KUSSIN, J.; SCHÜTZ, P.; Benchmark database on the evolution of two-phase flows in a vertical pipe Nuclear Engineering and Design 240 (2010) 2338–2346

[5] A. KAK, M. SLANEY, "Principles of Computerized Tomographic Imaging", IEEE Press, (New York, 1988).

[6] LIAO, Y.; LUCAS, D.; KREPPER, E.; SCHMIDTKE, M., "Development of a generalized coalescence and breakup closure for the inhomogeneous MUSIG model", Nuclear Engineering and Design (2011)